P CUC IVO ó4236/43: 4: 2"

Cpcn{ uku'qh'Y gm'Engct 'Dqwpf ct { 'O qf gnu'hqt 'yj g'Kpvgi tcvkqp'qh'WCU'kp'yj g'P CU"

Jason M. Upchurch, César A. Muñoz, Anthony J. Narkawicz,
James P. Chamberlain, and Maria C. Consiglio
Langley Research Center, Hampton, Virginia

NASA STI Program . . . in Profile

Ukpeg'ku'hqwpfkpi .'PCUC'jcu'dggp'fgfkecvgf ''vq'vjg''
cfxcpego gpv'qh'cgtqpcwkeu'cpf ''urceg'uekgpeg0'Vjg''
PCUC''uekgpvkhke''cpf ''vgej pkecn'kphqto cvkqp'*UVK+''
rtqitco ''rnc{u'c''mg{'rctv'kp'jgnrkpi 'PCUC'o ckpvckp''
vjku'ko rqtcpv'tqng0'

Vjg'PCUC''UVK'rtqitco ''qrgtcvgu'wpfgt'vjg''
cwurkegu'qh'vjg'Ci gpe{'Ej kgh'Kphqto cvkqp'Qhhkegt0'
Kv'eqnngevu.'qti cpk\gu.'rtqxkfgu'hqt'ctej kxkpi .'cpf ''
fkuugo kpcvgu'PCUCøu'UVK0'Vjg'PCUC'UVK''
rtqitco ''rtqxkfgu'ceeguu'vq'vjg'PCUC'Cgtqpcwkeu''
cpf ''Urceg'Fcvcdcug'cpf 'ku'rwdnke'kpvgthceg.'vjg''
PCUC'Vgej pkecn'Tgrqtv'Ugtxgt.'vjwu'rtqxkfkpi 'qpg''
qh'vjg'ncti gu'eqnngevkqpu'qh'cgtqpcwkecn'cpf 'urceg''
uekgpeg'UVK'kp'vjg'y qtnf0'Tguwnu'ctg'rwdnkuj gf 'kp''
dqvj 'pqp/PCUC'ej cppgnu'cpf 'd{'PCUC'kp'vjg''
PCUC'UVK'Tgrqtv'Ugtkgu.'y j kej 'kpenwfgu'vjg''
hqnnqy kpi 'tgrqtv'v{rgu<

- VGEJ P KECN'RWDNKECVKQP 0'Tgrqtvu'qh''
  eqo rngvgf 'tgugctej 'qt'c'o clqt'ukI pkhkecpv'rj cug''
  qh'tgugctej 'vj cv'rtgugpv'vj g'tguwnu'qh'PCUC''
  Rtqitco u'cpf 'kpenwfg'gzvgpukxg'fcvc'qt''
  vj gqtgvkecn'cpcn{uku0'Kpenwfgu'eqo rkncvkqpu'qh''
  ukI pkhkecpv'uekgpvkhke'cpf 'vgej pkecn'fcvc'cpf ''
  kphqto cvkqp'fggo gf 'vq'dg'qh'eqpvkpwkpi ''
  tghgtgpeg'xcnwg0PCUC'eqwpvgtrctv'qh'rggt/''
  tgxkgy gf 'hqto cn'rtqhguukqpcn'rcrgtu.'dwv''
  j cxkpi 'nguu'uvtkpi gpv'nko kcvkqpu'qp'o cpwuetkrv''
  ngpi vj 'cpf 'gzvgpv'qh'i tcrj ke'rtgugpvcvkqpu0'

- VGEJ P KECN'O GO QTCP FWO 0'Uekgpvkhke''
  cpf ''vgej pkecn'hkpfkpi u'vj cv'ctg'rtgnko kpct{'qt'qh''
  urgekcnk\gf 'kpvgtguv.'g0i 0.'swkem'tgngcug'tgrqtu.''
  y qtmkpi 'rcrgtu.'cpf 'dkdnki tcrj kgu'vj cv'eqpvckp''
  o kpko cn'cppqvcvkqp0'Fqgu'pqv'eqpvckp'gzvgpukxg''
  cpcn{uku0'

- EQP VTCEVQT 'TGRQTV0'Uekgpvkhke'cpf ''
  vgej pkecn'hkpfkpi u'd{'PCUC/urqpuqtgf ''
  eqpvtcevqtu'cpf 'i tcpvggu0'

- EQP HGTGP EG'RWDNKECVKQP 0''
  Eqnngevgf 'rcrgtu'htqo ''uekgpvkhke'cpf ''
  vgej pkecn'eqphgtgpegu.'u{o rqukc.'ugo kpctu.''
  qt'qvj gt'o ggvkpi u'urqpuqtgf 'qt'eq/''
  urqpuqtgf 'd{'PCUC0'

- URGEKCN'RWDNKECVKQP 0'Uekgpvkhke.''
  vgej pkecn'qt'j kuvqtkecn'kphqto cvkqp'htqo ''
  PCUC'rtqitco u.'rtqlgevu.'cpf 'o kuukqpu.''
  qhvgp'eqpegtpgf 'y kj 'uwdlgevu'j cxkpi ''
  uwduvcpvkcn'rwdnke'kpvgtguv0'

- VGEJ P KECN'VTCP UNCVKQP 0''
  Gpi nkuj /ncpi wci g'vtcpuncvkqpu'qh'hqtgki p''
  uekgpvkhke'cpf 'vgej pkecn'o cvgtkcn'rgtvkpgpv'vq''
  PCUCøu'o kuukqp0'

Urgekcnk\gf 'ugtxkegu'cnuq'kpenwfg'qti cpk\kpi ''
cpf 'rwdnkuj kpi 'tgugctej 'tguwnu.'fkuvtkdwvkpi ''
urgekcnk\gf 'tgugctej 'cppqwpego gpvu'cpf 'hggfu.''
rtqxkfkpi 'kphqto cvkqp'fguf'cpf 'rgtuqpcn'ugctej ''
uwr rqtv.'cpf 'gpcdnkpi 'fcvc'gzej ci g'ugtxkegu0'

Hqt'o qtg'kphqto cvkqp'cdqw'vj g'PCUC'UVK''
rtqitco .'ugg'vj g'hqnnqy kpi <

- Ceeguu'vj g'PCUC'UVK'rtqitco 'j qo g'rci g''
  cv'*http://www.sti.nasa.gov*

- G/o ckn'{qwt'swguvkqp'vq'*j gnr B uvk0pcuc0i qx*

- Hcz'{qwt'swguvkqp'vq'vj g'PCUC'UVK''
  Kphqto cvkqp'Fgum'cv'665/979/7: 25

- Rj qpg'vj g'PCUC'UVK'Kphqto cvkqp'Fgum'cv''
  665/979/7: 24

- Y tkvg'vq<
  """""""""UVK'Kphqto cvkqp'Fgum'
  """""""""P CUC'Egpvgt'hqt'CgtqUrceg'Kphqto cvkqp''
  """""""""9337'Uvcpfctf 'Ftkxg''
  """""""""J cpqxgt.'O F '43298/3542'

"

"

Cpcn{uku"qh"Y gm'Engct"Dqwpfct{"Oqfgnu"hqt"yj g"Kpvgitcvkqp"qh"WCU"kp"yj g"PCU""

0'

Jason M. Upchurch, César A. Muñoz, Anthony J. Narkawicz,
James P. Chamberlain, and Maria C. Consiglio
Langley Research Center, Hampton, Virginia

"

"

"

"

Lwpg"4236"

"

Abstract

The FAA-sponsored Sense and Avoid Workshop for Unmanned Aircraft Systems (UAS) defines the concept of *sense and avoid* for remote pilots as "the capability of a UAS to remain well clear from and avoid collisions with other airborne traffic." Hence, a rigorous definition of *well clear* is fundamental to any separation assurance concept for the integration of UAS into civil airspace. This paper presents a family of well-clear boundary models based on the TCAS II Resolution Advisory logic. Analytical techniques are used to study the properties and relationships satisfied by the models. Some of these properties are numerically quantified using statistical methods.

Acronyms

CAT   Collision Avoidance Threshold
CDF   Cumulative Distribution Function
NAS   National Airspace System
NMAC   Near Mid-Air Collision
RA   Resolution Advisory
SAA   Sense and Avoid
SST   Self-Separation Threshold
SSV   Self-Separation Volume
TCAS   Traffic Alerting and Collision Avoidance System
TCPA   Time to Closest Point of Approach
UAS   Unmanned Aircraft Systems

1 Introduction

One of the major challenges of integrating Unmanned Aircraft Systems (UAS) into the airspace system is the lack of an on-board pilot to comply with the legal requirement that pilots see and avoid other aircraft in their vicinity. To address this challenge, the final report of the FAA-sponsored Sense and Avoid (SAA) Workshop for Unmanned Aircraft Systems [2] defines the concept of *sense and avoid* for remote UAS pilots as "the capability of a UAS to remain well clear from and avoid collisions with other airborne traffic." Under this definition, a rigorous definition of well clear becomes fundamental to any sense and avoid concept that involves UAS.

NASA's Unmanned Aircraft Systems Integration in the National Airspace System (UAS in the NAS) project aims at conducting research towards the integration of civil UAS into non-segregated airspace operations. As part of this project, NASA has developed a sense and avoid concept for UAS that extends the concept outlined by the SAA Workshop [1]. The NASA concept includes a volume, namely the Self Separation Volume (SSV), located between the Collision Avoidance Threshold (CAT), defined by collision avoidance systems, and the Self-Separation Threshold (SST), defined by self-separation systems [2]. The SSV represents a well-clear boundary where aircraft inside the SSV are considered to be in well-clear violation. This volume is intended to be large enough to avoid safety concerns for controllers and see-and-avoid pilots, but small enough to avoid disruptions to traffic flow. A key characteristic of NASA's concept is that the SSV is a conservative extension of the CAT defined by the Traffic Alerting and Collision Avoidance System (TCAS).

TCAS is a family of airborne devices that are designed to reduce the risk of mid-air collisions between aircraft equipped with operating transponders [10]. TCAS II, the current generation of TCAS devices, is mandated in the US for aircraft with greater than 30 seats or a maximum takeoff weight greater than 33,000 pounds. Although it is not required, TCAS II is also installed on many turbine-powered general aviation aircraft. Version 7.0 is the current operationally-mandated version of TCAS II, and Version 7.1 has been standardized [8]. In contrast to TCAS I, the

first generation of TCAS devices, TCAS II provides *resolution advisories* (RAs). RAs are visual and vocalized alerts that direct pilots to maintain or increase vertical separation with intruders that are considered collision threats. TCAS II resolution advisories can be *corrective* or *preventive* depending on whether the pilot is expected to change or maintain the aircraft's current vertical speed. Corrective RAs are particularly disruptive to the air traffic system since they may cause drastic evasive maneuvers. For this reason, they are intended as a last resort maneuver when all other means of separation have failed.

The core of the TCAS II RA logic is a test that checks distance and time variables for the horizontal and vertical dimensions against a set of pre-defined threshold values. To ensure interoperability between NASA's SAA concept and TCAS, the mathematical definition of the volume SSV is based on the TCAS II Resolution Advisory Logic [5]. The definition of SSV follows the same logic, but uses different thresholds that conservatively extends the collision avoidance threshold provided by TCAS. This paper further generalizes the definition of the well-clear violation volume presented in [5] and presents a family of mathematical well-clear boundary models that are all based on the TCAS II RA logic. Formal and statistical techniques are used to study properties of this family of models.

The formal development presented in this paper is part of the NASA's Airborne Coordinated Resolution and Detection (ACCoRD) mathematical framework, which is electronically available from `http://shemesh.larc.nasa.gov/people/cam/ACCoRD`. All theorems in this paper have been formally verified in the Prototype Verification System (PVS) [7], an automated theorem prover.

2 Distance and Time Variables

Distance and time variables are important elements of any separation assurance concept. These variables are functions over the aircraft current states which are compared against distance and time thresholds. Many conflict detection and resolution systems rely on the time of closest point of approach and the distance at that time as their main time and distance variables [4]. This section describes some additional distance and time variables that are particularly relevant to the definition of a well-clear boundary model.

This paper assumes that accurate aircraft surveillance information is available as horizontal and vertical components in a three-dimensional (3-D) airspace. Letters in **bold-face** denote two-dimensional (2-D) vectors. Vector operations such as addition, subtraction, scalar multiplication, dot product, i.e., $\mathbf{s} \cdot \mathbf{v} \equiv s_x v_x + s_y v_y$, the square of a vector, i.e., $\mathbf{s}^2 \equiv \mathbf{s} \cdot \mathbf{s}$, and the norm of a vector, i.e., $\|\mathbf{s}\| \equiv \sqrt{\mathbf{s}^2}$, are defined in a 2-D Euclidean geometry. Furthermore, the expression $\mathbf{v}^\perp$ denotes a particular 2-D right-perpendicular vector of $\mathbf{v}$, i.e., $\mathbf{v}^\perp \equiv (v_y, -v_x)$, and $\mathbf{0}$ denotes the 2-D vector whose components are 0, i.e., $\mathbf{0} \equiv (0, 0)$.

The mathematical models presented in this paper consider two aircraft referred to as the *ownship* and the *intruder* aircraft. For the ownship, the current horizontal position and velocity are denoted $\mathbf{s}_o$ and $\mathbf{v}_o$, respectively. Its altitude and vertical speed are denoted s_{oz} and v_{oz}, respectively. Similarly, the horizontal position and

velocity of the intruder aircraft are denoted $\mathbf{s}_i$ and $\mathbf{v}_i$, respectively, and its vertical altitude and speed are denoted s_{iz} and v_{iz}, respectively. As it simplifies the mathematical development, this paper uses a relative coordinate system where the intruder is static at the center of the coordinate system. In this relative system, $\mathbf{s} = \mathbf{s}_o - \mathbf{s}_i$ and $\mathbf{v} = \mathbf{v}_o - \mathbf{v}_i$ represent the horizontal relative position and velocity of the aircraft, respectively. Furthermore, $s_z = s_{oz} - s_{iz}$ and $v_z = v_{oz} - v_{iz}$ represent the vertical relative position and speed of the aircraft, respectively.

Assuming constant relative horizontal velocity $\mathbf{v}$, the horizontal range between the aircraft at any time t is given by

$$r(t) \equiv \|\mathbf{s} + t\mathbf{v}\| = \sqrt{\mathbf{s}^2 + 2t(\mathbf{s} \cdot \mathbf{v}) + t^2 \mathbf{v}^2}. \tag{1}$$

The time of horizontal closest point of approach, denoted t_{cpa}, is the time t that satisfies $\dot{r}(t) = 0$, i.e., $t = -\frac{\mathbf{s} \cdot \mathbf{v}}{\mathbf{v}^2}$. The dot product $\mathbf{s} \cdot \mathbf{v}$ characterizes whether the aircraft are horizontally diverging, i.e., $\mathbf{s} \cdot \mathbf{v} > 0$, or horizontally converging, i.e., $\mathbf{s} \cdot \mathbf{v} < 0$. By convention, t_{cpa} is defined as 0 when $\mathbf{v} = \mathbf{0}$. Hence, t_{cpa} is formally defined as

$$t_{\text{cpa}}(\mathbf{s}, \mathbf{v}) \equiv \begin{cases} -\frac{\mathbf{s} \cdot \mathbf{v}}{\mathbf{v}^2} & \text{if } \mathbf{v} \neq \mathbf{0}, \\ 0 & \text{otherwise.} \end{cases} \tag{2}$$

It is noted that $t_{\text{cpa}}(\mathbf{s}, \mathbf{v}) > 0$ when the aircraft are horizontally converging, $t_{\text{cpa}}(\mathbf{s}, \mathbf{v}) < 0$ when the aircraft are horizontally diverging, and $t_{\text{cpa}}(\mathbf{s}, \mathbf{v}) = 0$ when the aircraft are neither converging or diverging. The distance at time of closest point of approach is defined as

$$d_{\text{cpa}}(\mathbf{s}, \mathbf{v}) \equiv r(t_{\text{cpa}}(\mathbf{s}, \mathbf{v})) = \|\mathbf{s} + t_{\text{cpa}}(\mathbf{s}, \mathbf{v})\mathbf{v}\|. \tag{3}$$

In the vertical dimension, assuming constant relative vertical speed, the relative altitude between the aircraft at any time t is given by

$$r_z(t) \equiv |s_z + tv_z|. \tag{4}$$

The time to co-altitude t_{coa} is the time t that satisfies $r_z(t) = 0$, i.e, $t = -\frac{s_z}{v_z}$. Similar to the horizontal case, the product $s_z v_z$ characterizes whether the aircraft are vertically diverging, i.e., $s_z v_z > 0$, or vertically converging, i.e., $s_z v_z < 0$. This paper defines time to co-altitude as -1 when the aircraft are not vertically converging. Therefore,

$$t_{\text{coa}}(s_z, v_z) \equiv \begin{cases} -\frac{s_z}{v_z} & \text{if } s_z v_z < 0, \\ -1 & \text{otherwise.} \end{cases} \tag{5}$$

Formula (5) is well defined since $s_z v_z < 0$ implies that $v_z \neq 0$.

2.1 Horizontal Time Variables

A (horizontal) time variable is a function that maps a relative horizontal position and velocity into a real number. This real number is negative when the aircraft are horizontally diverging. When the real number is non-negative, this number represents a time that, in a separation assurance logic, is intended to be compared

against a time threshold. In this paper, the time threshold is called `TTHR`. An example of a time variable that is used in conflict detection logics is t_{cpa} [4].

The time variable used in earlier versions of the TCAS detection logic is called *tau*, denoted τ [8]. Tau estimates t_{cpa}, but is less demanding on sensor and surveillance technology than t_{cpa}. Indeed, τ is simply defined as range over closure rate, where closure rate is the negative of the range rate, i.e., $\tau = -\frac{r(0)}{\dot{r}(0)} = -\frac{\|\mathbf{s}\|}{\frac{\mathbf{s}\cdot\mathbf{v}}{\|\mathbf{s}\|}} = -\frac{\mathbf{s}^2}{\mathbf{s}\cdot\mathbf{v}}$. This paper defines τ as -1 when the aircraft are not horizontally converging. Formally,

$$\tau(\mathbf{s}, \mathbf{v}) \equiv \begin{cases} -\frac{\mathbf{s}^2}{\mathbf{s}\cdot\mathbf{v}} & \text{if } \mathbf{s}\cdot\mathbf{v} < 0, \\ -1 & \text{otherwise.} \end{cases} \tag{6}$$

For a limited number of scenarios, the values of τ and t_{cpa} coincide. However, in most scenarios, the value of τ tends toward infinity as the aircraft approach the closest point of approach. In general, τ is a good approximation of t_{cpa}, but only for large values. For that reason, TCAS II uses a modified variant of τ called *modified tau*, denoted τ_{mod} [8]. Modified tau provides a better estimation of t_{cpa} and has a more desirable behavior than τ in the proximity of the closest point of approach. In [3], modified tau is defined such that $\tau_{\text{mod}} = -\frac{r(0)^2 - \text{DTHR}^2}{\dot{r}(0)} = \frac{\text{DTHR}^2 - \mathbf{s}^2}{\mathbf{s}\cdot\mathbf{v}}$. Similar to τ, τ_{mod} is defined as -1 when the aircraft are not horizontally converging, i.e.,

$$\tau_{\text{mod}}(\mathbf{s}, \mathbf{v}) \equiv \begin{cases} \frac{\text{DTHR}^2 - \mathbf{s}^2}{\mathbf{s}\cdot\mathbf{v}} & \text{if } \mathbf{s}\cdot\mathbf{v} < 0, \\ -1 & \text{otherwise.} \end{cases} \tag{7}$$

The definition of τ_{mod} in Formula (7) depends on `DTHR`, which is a horizontal distance threshold. This threshold is called *DMOD* in the TCAS II RA logic, and its actual value depends on a sensitivity level based on the ownship's altitude [8].

In [6], a time variable called *time to entry point*, denoted t_{ep}, is proposed. Time to entry point is defined as the time to loss of horizontal separation with respect to `DTHR` assuming straight-line aircraft trajectories. Similar to t_{cpa}, t_{ep} decreases linearly over time. Time to entry point is formally defined as

$$t_{\text{ep}}(\mathbf{s}, \mathbf{v}) \equiv \begin{cases} \Theta(\mathbf{s}, \mathbf{v}, \text{DTHR}, -1) & \text{if } \mathbf{s}\cdot\mathbf{v} < 0 \text{ and } \Delta(\mathbf{s}, \mathbf{v}, \text{DTHR}) \geq 0, \\ -1 & \text{otherwise,} \end{cases} \tag{8}$$

where

$$\Theta(\mathbf{s}, \mathbf{v}, D, \epsilon) \equiv \frac{-\mathbf{s}\cdot\mathbf{v} + \epsilon\sqrt{\Delta(\mathbf{s}, \mathbf{v}, D)}}{\mathbf{v}^2}, \tag{9}$$

$$\Delta(\mathbf{s}, \mathbf{v}, D) \equiv D^2\mathbf{v}^2 - (\mathbf{s}\cdot\mathbf{v}^\perp)^2. \tag{10}$$

The function Θ is only defined when $\mathbf{v} \neq \mathbf{0}$ and $\Delta(\mathbf{s}, \mathbf{v}, D) \geq 0$. In this case, it computes the times when the aircraft will lose separation, if $\epsilon = -1$, or regain separation, if $\epsilon = 1$, with respect to D. When the aircraft are not horizontally converging or $\Delta(\mathbf{s}, \mathbf{v}, D) < 0$, time to entry point is defined as -1. Formula (8) is well defined since the condition $\mathbf{s}\cdot\mathbf{v} < 0$ guarantees that $\mathbf{v} \neq \mathbf{0}$.

2.2 Properties of Horizontal Time Variables

A useful property of a time variable is *symmetry*. A time variable t_{var} is said to be symmetric if and only for all $\mathbf{s}, \mathbf{v}$,

$$t_{\mathrm{var}}(\mathbf{s}, \mathbf{v}) = t_{\mathrm{var}}(-\mathbf{s}, -\mathbf{v}). \tag{11}$$

Symmetry guarantees that in a pairwise scenario both the ownship and intruder aircraft compute the same value for the time variable. Hence, checking a symmetric time variable against a given time threshold returns the same Boolean value for both aircraft.

Theorem 1. *The time variables τ, t_{cpa}, τ_{mod}, and t_{ep} are symmetric.*

It is possible to define time variables that are not symmetric. For instance, a time variable that computes the first time when the intruder aircraft enters an elliptical area aligned to the ownship trajectory is not symmetric for every scenario. However, any time variable can be transformed into a symmetric one by using min and max operators. For instance, the time variables $\min(t_{\mathrm{var}}(\mathbf{s}, \mathbf{v}), t_{\mathrm{var}}(-\mathbf{s}, -\mathbf{v}))$ and $\max(t_{\mathrm{var}}(\mathbf{s}, \mathbf{v}), t_{\mathrm{var}}(-\mathbf{s}, -\mathbf{v}))$ are symmetric for any time variable t_{var}.

Figure 1 shows a graph of τ, t_{ep}, τ_{mod}, and t_{cpa} versus time for an initial scenario where the ownship and intruder aircraft are located at $(0 \text{ nmi}, -3.25 \text{ nmi})$ and $(-6.25 \text{ nmi}, 0.25 \text{ nmi})$, respectively, flying at co-altitude. Furthermore, the ownship ground speed is 150 kn, heading 53°, and the intruder ground speed is 350 kn, heading 90°.[1] In this scenario, the distance threshold `DTHR` used in the definition of τ_{mod} and t_{ep} is 1 nmi. This scenario illustrates that while t_{ep}, τ_{mod}, and t_{cpa} decrease over time, the time variable τ decreases up to some point, but then it abruptly increases in the vicinity of the closest point of approach. Moreover, when these time variables are checked against a time threshold `TTHR`, represented by the horizontal line at 30 seconds, the time variable t_{ep} crosses the time threshold first, followed by τ_{mod}, then t_{cpa}, and finally τ. Interestingly, this ordering property holds for any converging scenario and any choice of common threshold values.

Theorem 2. *Let $\mathbf{s}, \mathbf{v}$ be such that $\mathbf{s} \cdot \mathbf{v} < 0$, $\|\mathbf{s}\| > DTHR$, and $d_{cpa}(\mathbf{s}, \mathbf{v}) \leq DTHR$, i.e., the aircraft are horizontally converging, are outside the distance threshold DTHR, and their distance at time of closest point of approach is less than or equal to DTHR. Then the following inequalities hold*

$$t_{ep}(\mathbf{s}, \mathbf{v}) \leq \tau_{mod}(\mathbf{s}, \mathbf{v}) \leq t_{cpa}(\mathbf{s}, \mathbf{v}) \leq \tau(\mathbf{s}, \mathbf{v}). \tag{12}$$

3 A Family of Well-Clear Boundary Models

A well-clear boundary specifies the set of aircraft states that are considered to be in well-clear violation. Following the TCAS detection logic, the well-clear boundary models in this paper are specified by a logical condition that simultaneously checks

---

[1]Aircraft headings are measured in true north clockwise convention, i.e., 0° points to the north and degrees are positive in clockwise direction.

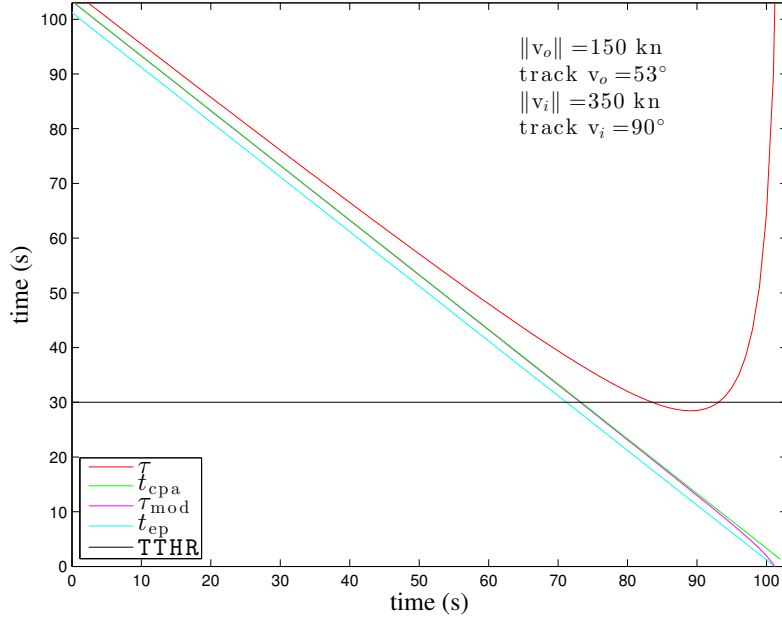Figure 1: Time vs. τ, t_{cpa}, τ_{mod}, t_{ep}

horizontal and vertical violations. A horizontal violation occurs if the current range is less than a given horizontal distance threshold `DTHR`. A horizontal violation also occurs if distance at time of closest point of approach is less than `DTHR` and a given time variable t_{var} is less than a given time threshold `TTHR`. In the vertical dimension, a similar comparison is made. Vertical well clear is violated if the relative altitude is less than a given altitude threshold `ZTHR` or if the time to co-altitude is less than a given vertical time threshold `TCOA`. The distance and altitude thresholds are considered to be positive numbers, i.e., `DTHR` > 0 and `ZTHR` > 0. The time thresholds are considered to be non-negative, i.e., `TTHR` ≥ 0 and `TCOA` ≥ 0. Formally, this well-clear violation condition can be denoted as follows.

$$
\begin{aligned}
WCV_{t_{\mathrm{var}}}(\mathbf{s}, s_z, \mathbf{v}, v_z) \equiv\ &\texttt{Horizontal\_WCV}_{t_{\mathrm{var}}}(\mathbf{s}, \mathbf{v}) \text{ and} \\
&\texttt{Vertical\_WCV}(s_z, v_z),
\end{aligned}
\tag{13}
$$

where

$$
\begin{aligned}
\texttt{Horizontal\_WCV}_{t_{\mathrm{var}}}(\mathbf{s}, \mathbf{v}) \equiv\ &\|\mathbf{s}\| \leq \texttt{DTHR or} \\
&(d_{\mathrm{cpa}}(\mathbf{s}, \mathbf{v}) \leq \texttt{DTHR and } 0 \leq t_{\mathrm{var}}(\mathbf{s}, \mathbf{v}) \leq \texttt{TTHR}), \\
\texttt{Vertical\_WCV}(s_z, v_z) \equiv\ &|s_z| \leq \texttt{ZTHR or } 0 \leq t_{\mathrm{coa}}(s_z, v_z) \leq \texttt{TCOA}.
\end{aligned}
$$

The logical condition $WCV_{t_{\mathrm{var}}}$ defines a family of well-clear boundary models where t_{var} can be instantiated with any time variable, and `DTHR`, `TTHR`, `ZTHR`, and `TCOA` are set to threshold values of interest. The fact that the time thresholds `TTHR` and `TCOA` can be zero allows for the definition of well-clear boundary models that do not depend on time thresholds. For instance, when `TTHR` $= 0$ and `TCOA` $= 0$, $WCV_{t_{\mathrm{cpa}}}$ specifies the loss of separation condition for a cylindrical volume of radius

6

`DTHR` and half-height `ZTHR` around one of the aircraft. Indeed, in this case, $WCV_{t_{\mathrm{cpa}}}$ is logically equivalent to the logical condition $\|\mathbf{s}\| \leq \texttt{DTHR}$ and $|s_z| \leq \texttt{ZTHR}$.

The TCAS II RA core logic provided in [5] is used by $WCV_{\tau_{\mathrm{mod}}}$, where `DTHR`, `TTHR`, `ZTHR`, and `TCOA` are set to the TCAS II thresholds DMOD, TAU, ZTHR, and TAU, respectively. The actual values of these thresholds are given in a table indexed by sensitivity levels based on the ownship's altitude [8]. In the TCAS II RA logic, the logical condition $d_{\mathrm{cpa}}(\mathbf{s}, \mathbf{v}) \leq \texttt{DTHR}$ in the horizontal check is called *horizontal miss-distance filter* and, in that condition, `DTHR` is set to the miss-horizontal distance threshold HMD, which is equal to DMOD. The well-clear boundary model defined in [6] is obtained by $WCV_{t_{\mathrm{ep}}}$, where $\texttt{TCOA} = \texttt{TTHR}$.

Henceforth, the well-clear models specified by WCV_{τ}, $WCV_{t_{\mathrm{cpa}}}$, $WCV_{\tau_{\mathrm{mod}}}$, and $WCV_{t_{\mathrm{ep}}}$ will be referred to as WC_TAU, WC_TCPA, WC_TAUMOD, and WC_TEP, respectively. The rest of this section studies properties and relations satisfied by these models.

3.1 Symmetry

A well-clear boundary model specified by $WCV_{t_{\mathrm{var}}}$, for a given time variable t_{var}, is *symmetric* if and only if

$$WCV_{t_{\mathrm{var}}}(\mathbf{s}, s_z, \mathbf{v}, v_z) = WCV_{t_{\mathrm{var}}}(-\mathbf{s}, -s_z, -\mathbf{v}, -v_z). \tag{14}$$

In other words, in a symmetric well-clear boundary model, both the ownship and intruder aircraft have the same perception of being well clear or not.

Theorem 3 (Symmetry)**.** *If t_{var} is symmetric, the well-clear boundary model specified by $WCV_{t_{var}}$ is symmetric. Hence, by Theorem 1, the well-clear boundary models WC_TAU, WC_TCPA, WC_TAUMOD, and WC_TEP are symmetric for any choice of threshold values `DTHR`, `TTHR`, `ZTHR`, and `TCOA`.*

3.2 Inclusion

Figure 2 illustrates the violation areas for the well-clear boundary models WC_TAU, WC_TAUMOD, WC_TCPA, and WC_TEP for the scenario of Figure 1. The threshold values used in this scenario are $\texttt{DTHR} = 1$ nmi, $\texttt{TTHR} = \texttt{TCOA} = 30$ s, and $\texttt{ZTHR} = 475$ ft. The violation areas in these figures are similar to the conflict contours proposed in [9]. The points in these areas represent future locations of the ownship where a well-clear violation will occur assuming that the intruder aircraft continues its current trajectory and the ownship either continues its current trajectory or instantaneously changes its direction but keeps its ground speed.

Figure 3 overlays the violation areas for the four boundary models. This figure illustrates that for a common set of threshold values, the violation area of WC_TAU is included in the violation area of WC_TCPA, which is included in the violation area of WC_TAUMOD, which is included in the violation area of WC_TEP. Theorem 4 below states that this inclusion property always holds for any encounter geometry and choice of common threshold values. Theorem 4 is a consequence of Theorem 2.
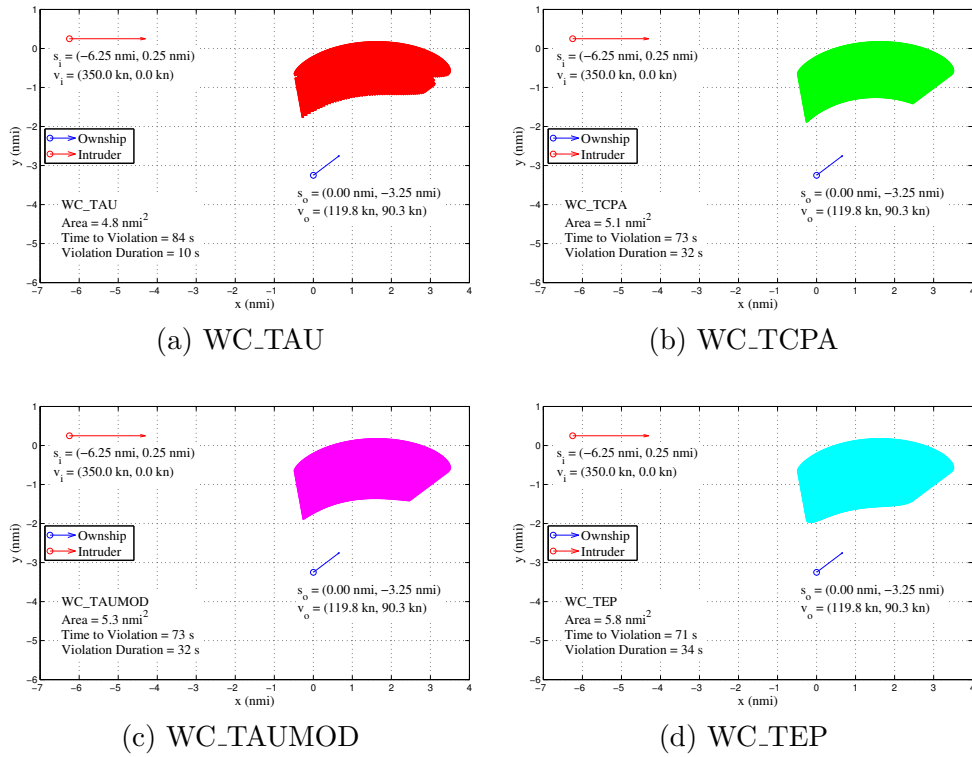
(a) WC_TAU

(b) WC_TCPA

(c) WC_TAUMOD

(d) WC_TEP

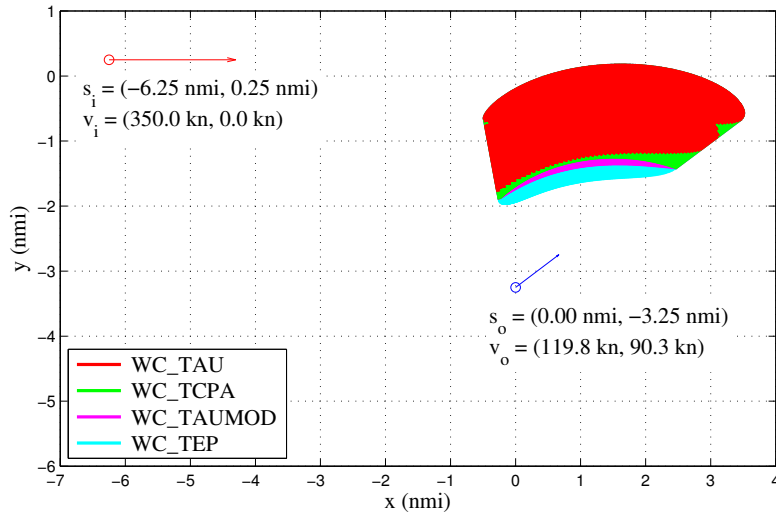Figure 2: Violation areas for scenario of Figure 1

Figure 3: Overlay of violation areas for scenario of Figure 1

Theorem 4 (Inclusion). *For all* $\mathbf{s}, s_z, \mathbf{v}, v_z$ *and choice of threshold values* `DTHR`, `TTHR`, `ZTHR`, *and* `TCOA`, *the following implications hold*

(i) $WCV_\tau(\mathbf{s}, s_z, \mathbf{v}, v_z) \implies WCV_{t_{cpa}}(\mathbf{s}, s_z, \mathbf{v}, v_z),$

(ii) $WCV_{t_{cpa}}(\mathbf{s}, s_z, \mathbf{v}, v_z) \implies WCV_{\tau_{mod}}(\mathbf{s}, s_z, \mathbf{v}, v_z),$ *and*

(iii) $WCV_{\tau_{mod}}(\mathbf{s}, s_z, \mathbf{v}, v_z) \implies WCV_{t_{ep}}(\mathbf{s}, s_z, \mathbf{v}, v_z).$

A key consequence of Theorem 4 is that of the four well-clear boundary models, WC_TEP provides the most conservative safety margins in terms of having the largest violation area and the earliest time whereby a well-clear violation is defined to occur. The remaining models can be ordered from most conservative to least conservative as WC_TAUMOD, WC_TCPA, and WC_TAU.

3.3 Local Convexity

As illustrated by Figure 2, the violation areas are not geometrically convex. However, Figures 2(b)-(d) show that from the point of view of the ownship, any ray that points towards the violation area has only one intersecting segment. This property is referred to as *local convexity*. It can be verified by inspection of Figure 2(a) that this property does not always hold in the case of WC_TAU. A formal definition of local convexity follows.

Definition 1 (Local convexity). *A well-clear boundary model specified by* $WCV_{t_{var}}$, *for a given time variable* t_{var}, *is* locally convex *if and only if there are no times* $0 \le t_1 \le t_2 \le t_3 \le T$ *such that*

1. *the aircraft are not well clear at time* t_1, *i.e.,* $WCV_{t_{var}}(\mathbf{s} + t_1\mathbf{v}, s_z + t_1 v_z, \mathbf{v}, v_z),$

2. *the aircraft are well clear at time* t_2, *i.e.,* $\neg WCV_{t_{var}}(\mathbf{s} + t_2\mathbf{v}, s_z + t_2 v_z, \mathbf{v}, v_z),$ *and*

3. *the aircraft not well clear at time* t_3, *i.e.,* $WCV_{t_{var}}(\mathbf{s} + t_3\mathbf{v}, s_z + t_3 v_z, \mathbf{v}, v_z).$

Thus, a well-clear boundary model is locally convex if for any ownship straight-line trajectory there is at most one time interval where the aircraft are not well clear.

Theorem 5. *For any choice of threshold values, the well-clear boundary models WC_TCPA, WC_TAUMOD, and WC_TEP are locally convex.*

As illustrated by Figure 2(a), the well-clear boundary model WC_TAU is not locally convex for all choices of threshold values. In particular, it can be seen in Figure 1, assuming straight-line trajectories, that for the same encounter scenario the aircraft will have a well-clear violation at 91 s, 7 seconds later they will be well clear, and 7 seconds after being well clear, they will have another well-clear violation.

Theorem 6. *For some choices of threshold values, the well-clear boundary model WC_TAU is not locally convex.*
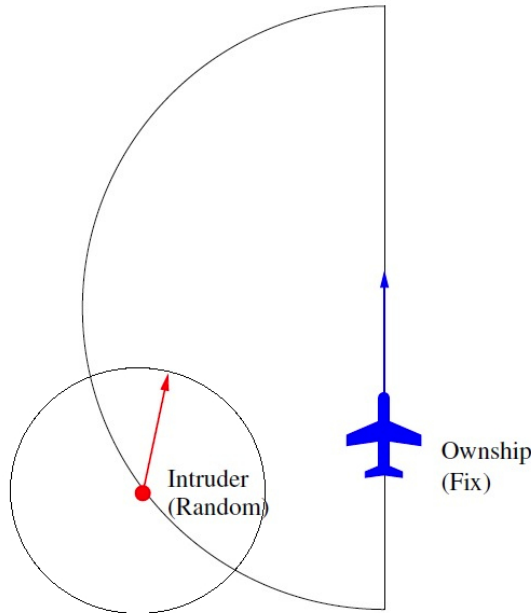
9

Figure 4: Depiction of a randomly-generated encounter (top view)

4 Preliminary Statistical Analysis of Well-Clear Boundary Models

This section presents a preliminary statistical analysis of the well-clear models defined in Section 3, with the goal of characterizing the models in terms of relevant metrics. In particular, the metrics used for comparison are: (1) the violation areas associated with well-clear violations, and (2) the times when a well-clear violation first occurs. These metrics serve to validate the inclusion relation given by Theorem 4.

4.1 Random Encounter Generation

The encounter space used in the statistical analysis presented in this section consists of a half cylinder of radius, R, and height, h. The top view of this situation is shown in Figure 4 for an arbitrary encounter, and the three-dimensional view is shown in Figure 5 for a different arbitrary encounter.

The ownship initial position is chosen to be constant as $\mathbf{s}_o = (0, -\frac{R}{2})$ and $s_{oz} = \frac{h}{2}$. The ownship horizontal velocity component $\mathbf{v}_o$ is randomly chosen from a Burr distribution with parameters $\alpha = 37.0896, c = 2.6351, k = 1.00604$ and is intended to be representative of a fixed-wing UAS, based on the distribution of the velocity characteristics of 849 fixed-wing UAS [11]. The ownship vertical velocity component v_{oz} is chosen to be zero. The motivation for this particular encounter space is to create stress scenarios whereby encounters are biased to result in violations, where the violations cover a broad range of encounter geometries. The details of the encounter space parameters follow.
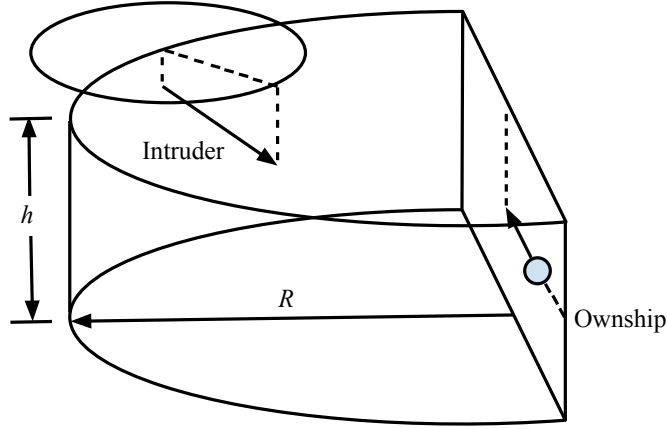
10

Figure 5: Depiction of a randomly-generated encounter (3-dimensional view)

The intruder initial position in the horizontal plane, $\mathbf{s}_i$, is randomly chosen from a uniform distribution to be on the left half cylinder circumference as shown in Figure 4. The intruder initial position in the vertical plane, s_{iz}, is chosen from a normal distribution having a mean of zero and a standard deviation of $\frac{h}{(2)(2.99)}$, where s_{iz} is set to be either $\frac{h}{2}$ or $-\frac{h}{2}$ if the random variable falls in the upper or lower tail of the distribution, respectively. The intruder initial horizontal velocity magnitude is chosen from the same distribution as the ownship. Furthermore, the intruder's horizontal velocity vector direction is chosen from a uniform distribution to terminate on the small circle shown in Figures 4 and 5. The intruder vertical velocity magnitude is randomly chosen from a normal distribution having a mean of zero and a standard deviation of $\frac{v_{iz,\mathrm{max}}}{(2)(2.99)}$, where v_{iz} is set to be either $v_{iz,\mathrm{max}}$ or $-v_{iz,\mathrm{max}}$ if the random variable falls in the upper or lower tail of the distribution, respectively.

4.2 Computation of Violation Area

Given a set of initial position and velocity states for the ownship and intruder, a well-clear violation area is generated by first indexing the ownship trajectory through 360 degrees over N steps while holding $\|\mathbf{v}_o\|$ and v_{oz} constant, that is, the ownship trajectory is swept around a cone of constant height, where each of the N trajectories is assumed to remain constant. Next, for each of the N ownship trajectories generated, the time interval for any well-clear violation, $[t_{\mathrm{in}}, t_{\mathrm{out}}]$, is computed for the given trajectory. Then, the associated line segment in three-dimensional space is projected onto a two-dimensional plane containing the ownship initial position. As discussed in Section 3.3, the WC_TAU model is not locally convex. Hence, there may be aircraft states that yield multiple instances of t_{in} and t_{out} for a given trajectory. In such cases, each segment is considered separately. The resulting geometry for an example encounter are illustrated in Figure 6.

In the analysis presented in this paper, a violation area associated with a well-clear violation is considered to be such a projection into two dimensions. It can be verified that for the special case of $v_{oz} = 0$, the height of the cone collapses to zero,
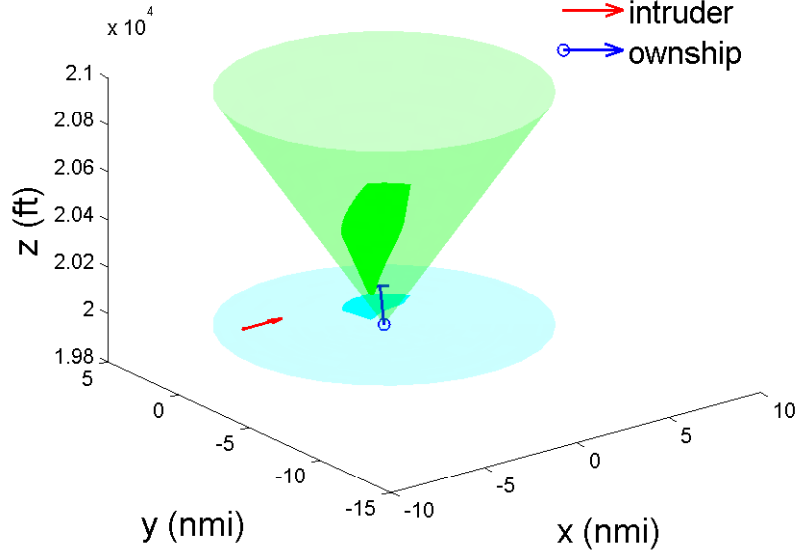
11

Figure 6: Projection of three-dimensional violation volume into two dimensions

and the original and projected volumes coincide.

The area of the two-dimensional violation area is computed as follows. First, consider a differential area in the polar coordinate system given by

$$\mathrm{d}A = \frac{1}{2}(\bar{r}^2 - \underline{r}^2)\mathrm{d}\theta, \tag{15}$$

where $\underline{r}$ corresponds to the distance from the ownship initial position to the position at time t_{in}, $\bar{r}$ corresponds to the distance from the ownship initial position to the position at time t_{out}, and $\mathrm{d}\theta$ corresponds to the differential angle between adjacent ownship trajectories, that is,

$$\mathrm{d}\theta = \frac{2\pi}{N}.$$

Thus, the analytical violation area is determined as

$$\lim_{N \to \infty} \sum_{k=1}^{N} \sum_{i=1}^{M} \frac{\pi}{N}(\bar{r}_{i,k}^2 - \underline{r}_{i,k}^2), \tag{16}$$

where M represents the number of violation regions on the kth trajectory, and if a well-clear violation does not occur for the kth trajectory then $\underline{r}_{i,k}$ and $\bar{r}_{i,k}$ are defined to be zero for that trajectory.

The algorithm implemented to compute the numerical approximation of the violation area is given by

$$\sum_{k=1}^{N^*} \sum_{i} \frac{\pi}{N^*}(\bar{r}_{i,k}^2 - \underline{r}_{j,k}^2), \tag{17}$$
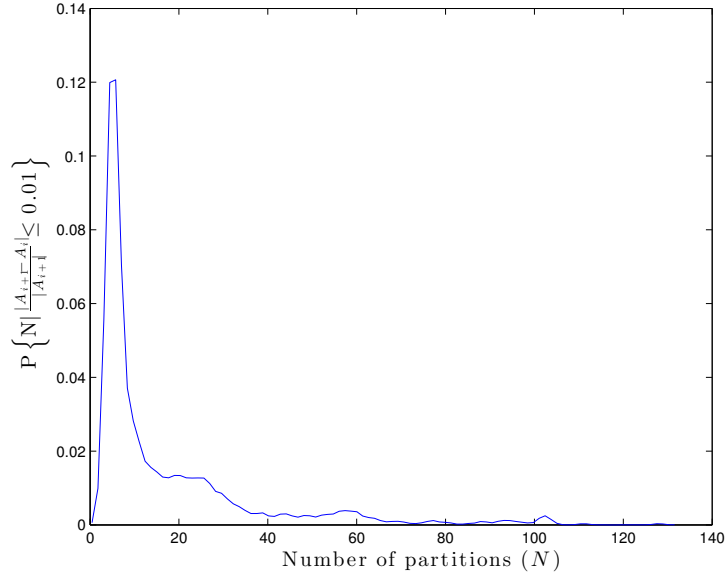
12

Figure 7: Estimate of probability density function of N for 1000 trials

where N^* denotes a particular choice for N. It can be verified that this estimate converges to the actual area as N^* approaches infinity.

The particular choice for N^* used for the analysis in the remainder of this paper was arrived at through a Monte Carlo experiment which was run until 1000 random encounter trajectories resulting in well-clear violations were accumulated. For each well-clear violation, N was initialized with $N = 2$ and the corresponding violation area was calculated using Formula (17). The value of N was then incremented by one and the violation area recomputed. This process continued until the relative difference between the computed area and the previously-computed area was below 1%. Thus, the value of N for any randomly-generated encounter was chosen as the number of partitions that first satisfied the 1% condition. An estimate of the distribution of N for the 1000 well-clear violations is shown in Figure 7. This figure was used as a basis for choosing $N^* = 360$, which is assumed for the remainder of the analysis in this paper. Thus, the differential angle for the velocity sweep is necessarily $1°$.

4.3 Analysis

In the subsequent analysis, the choice is made to present comparisons of WC_TAU, WC_TCPA, and WC_TAUMOD relative to WC_TEP. That is, the analysis and metrics presented are with respect to WC_TEP. In particular, the two metrics used for the following discussion are: (1) the relative difference in violation areas,

determined as

$$\Delta A(t_{\text{var}}) = \frac{A(WCV_{t_{\text{ep}}}) - A(WCV_{\tau})}{A(WCV_{t_{\text{ep}}})}, \tag{18}$$

$$\Delta A(t_{\text{var}}) = \frac{A(WCV_{t_{\text{ep}}}) - A(WCV_{t_{\text{cpa}}})}{A(WCV_{t_{\text{ep}}})}, \tag{19}$$

$$\Delta A(t_{\text{var}}) = \frac{A(WCV_{t_{\text{ep}}}) - A(WCV_{\tau_{\text{mod}}})}{A(WCV_{t_{\text{ep}}})}, \tag{20}$$

and (2) the difference in time when a well-clear violation will first occur, determined as

$$\Delta t_{\text{in}}(t_{\text{var}}) = t_{\text{in}}(WCV_{t_{\text{ep}}}) - t_{\text{in}}(WCV_{\tau}), \tag{21}$$

$$\Delta t_{\text{in}}(t_{\text{var}}) = t_{\text{in}}(WCV_{t_{\text{ep}}}) - t_{\text{in}}(WCV_{t_{\text{cpa}}}), \tag{22}$$

$$\Delta t_{\text{in}}(t_{\text{var}}) = t_{\text{in}}(WCV_{t_{\text{ep}}}) - t_{\text{in}}(WCV_{\tau_{\text{mod}}}). \tag{23}$$

The statistical analysis of violation areas is obtained from a Monte Carlo simulation with 10,000 well-clear violations (i.e., greater than 10,000 trials). Each trial consisted of a random encounter scenario having the geometry discussed in Section 4.1. For each trial, if the random encounter resulted in a joint well-clear violation for all models, the corresponding areas were computed, followed by the relative area differences with respect to WC_TEP. This process was repeated until 10,000 joint well-clear violations were accumulated, and the cumulative distribution function (CDF) for WC_TAUMOD and WC_TCPA with respect to WC_TEP was then computed (see Formulas 18-20). Figure 8 shows the results of the Monte Carlo experiment, where the threshold values used for the simulation were TTHR = 30 s, DTHR = 1 nmi, and ZTHR = 475 ft. The preliminary analysis of the CDFs in Figure 8 reveal that: (1) the areas for WC_TAUMOD and WC_TEP differ by less than 25% in approximately 95% of the well-clear violations, (2) the areas for WC_TCPA and WC_TEP differ by as much as 55% in approximately 95% of the well-clear violations, and (3) the areas for WC_TAU and WC_TEP differ by as much as 70% in 95% of the well-clear violations. The Monte-Carlo results provide an experimental validation of the inclusion property discussed in Section 3.2.

The second metric used to analyze the well-clear models is t_{in}, the time when a well-clear violation first occurs (see Formulas 21-23). During the same Monte Carlo experiment previously discussed, if a joint well-clear violation for an initial set of randomly-generated ownship and intruder positions and velocities occurs, then the time when the well-clear violation occurs for each model is computed using only the initial positions and velocities. For each encounter resulting in a well-clear violation, the time difference with respect to WC_TEP is computed for WC_TAU, WC_TCPA, and WC_TAUMOD. Upon accumulation of 10,000 well-clear violations, the CDFs of the time difference in time were generated. The results of the Monte Carlo experiment are shown in Figure 9.

The CDFs in Figure 9 show that: (1) the difference between t_{in} for WC_TAUMOD and WC_TEP is limited to approximately 15 s, (2) the difference between t_{in} for
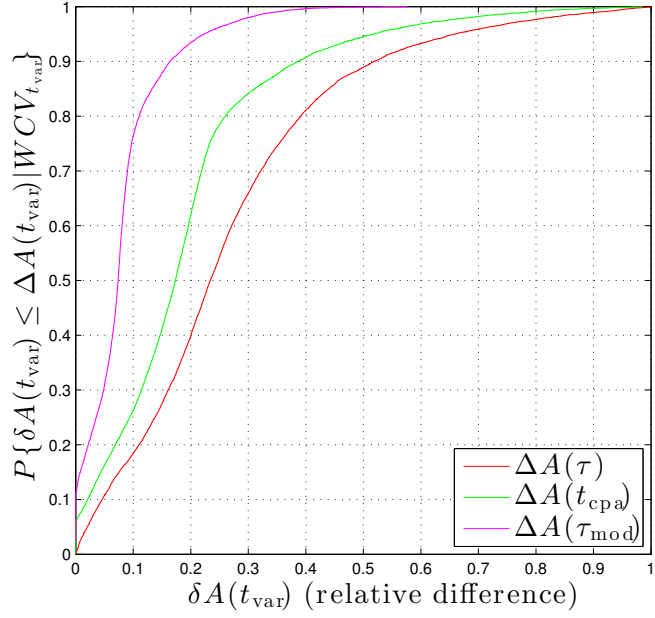
14

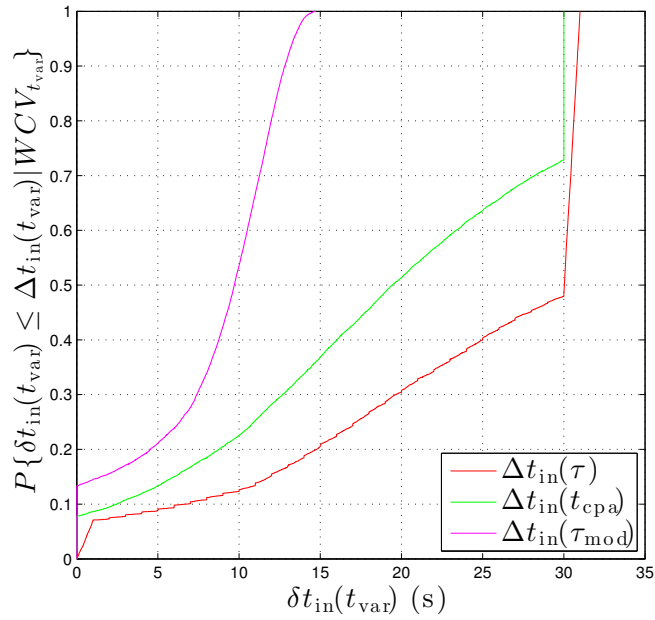Figure 8: CDF of relative difference in area with respect to WC_TEP

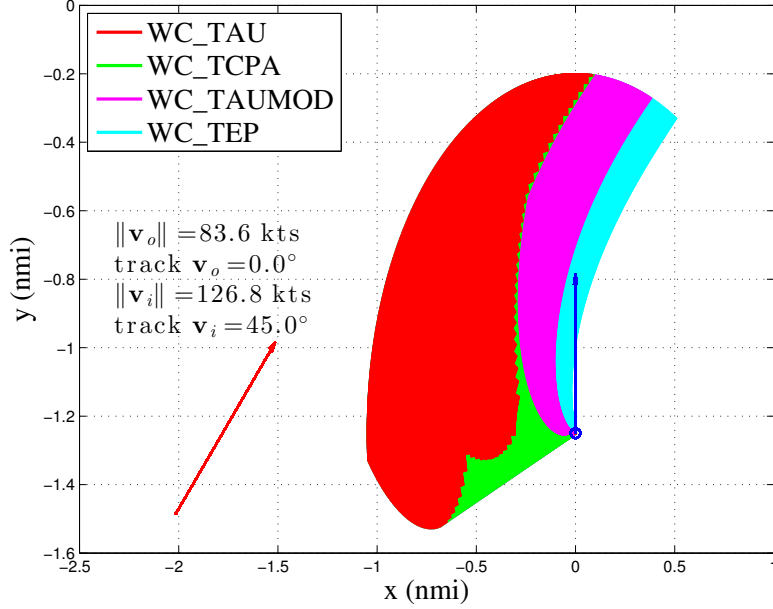Figure 9: CFD of absolute difference first time to violation with respect to WC_TEP

15

Figure 10: Encounter geometry of interest: large difference in t_{in}

WC_TCPA and WC_TEP is limited to exactly 30 s, which is `TTHR` for the experiment, and (3) the difference between t_{in} for WC_TAU and WC_TEP may slightly exceed the 30-second `TTHR`.

While Figures 8 and 9 provide a visual validation of the inclusion property, additional insight can be gained by considering some examples designed to illustrate the implications of each particular well-clear model. Figures 10 and 11 show two such examples.

Figure 10 shows an encounter geometry designed to illustrate a case when all of the well-clear models indicate a well-clear violation will occur at some time in the future given the initial ownship and intruder trajectories, yet a significant difference in t_{in} exists for each approach. In particular, the value for t_{in} for each model is:

1. WC_TAU 42 s,

2. WC_TCPA 41.7 s,

3. WC_TAUMOD 23.9 s,

4. WC_TEP 11.7 s.

Thus, the maximum Δt_{in} is WC_TEP $-$ WC_TAU $= 30.3$ s. This scenario depicts a situation where every model will eventually determine a well-clear violation exists for the current, constant-velocity trajectory, however there is a wide range in t_{in}, the time when such a violation first occurs. The figure also demonstrates another case of violation of the local convexity property for the WC_TAU model.
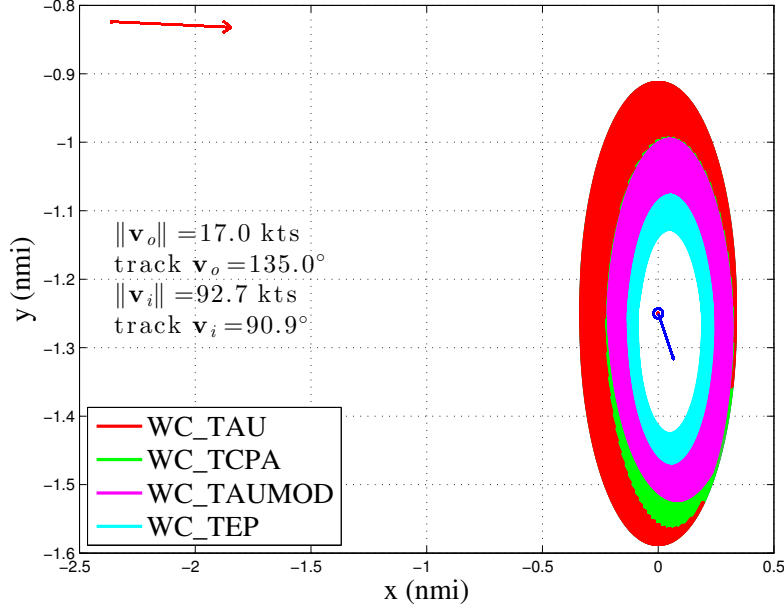
16

Figure 11: Encounter geometry of interest: non-agreement over $WCV_{t_{\mathrm{var}}}$

Figure 11 shows a case when all but one well-clear model results in a well-clear violation for the initial trajectory. In particular, WC_TCPA, WC_TAUMOD, and WC_TEP produce well-clear boundaries in any horizontal direction the ownship may travel, however, the WC_TAU model produces a region on the ownship's current trajectory in which the ownship may pass without incurring a well-clear violation. This example was selected to illustrate that there are other important, characterizing properties of the models appropriate for investigation beyond area and t_{in}. This paper does not present an extensive analysis of such considerations.

5   Conclusion

A family of well-clear boundary models is presented. This family generalizes the TCAS II Resolution Logic with different possible definitions of horizontal time variables including tau, time to closest point of approach, modified tau, and time to entry point. Analytical techniques are used to study the properties of this model. For instance, it has been formally proved that the well-clear model based on time to entry point is more conservative than tau, time to closest point of approach, and modified tau for any scenario and any common choice of threshold values. Furthermore, it is shown that all the models in this family are symmetric, i.e., the ownship and intruder aircraft have the same perception of being well-clear or not at any moment in time. Except for the model based on tau, all the models are locally convex meaning that there is at most one interval of time when the aircraft are not well-clear, assuming straight-line trajectories.

17

Some of these properties are validated through numerical quantification using statistical methods. In particular, random encounters are generated in Monte Carlo fashion, and distributions for area and t_{in} are determined for 10,000 data points. This analysis represents a preliminary look at some characterizing properties of the family of well-clear boundary models.

The mathematical development presented in this paper has been mechanically verified in the Prototype Verification System (PVS) [7]. This level of rigor is justified by the safety-critical nature of the well-clear concept to the integration of Unmanned Aircraft Systems in the the National Aerospace System.

References

1. María Consiglio, James Chamberlain, César Muñoz, and Keith Hoffler. Concept of integration for UAS operations in the NAS. In *Proceedings of 28th International Congress of the Aeronautical Sciences, ICAS 2012*, Brisbane, Australia, 2012.

2. FAA Sponsored Sense and Avoid Workshop. Sense and avoid (SAA) for Unmanned Aircraft Systems (UAS), October 2009.

3. Jonathan Hammer. Horizontal miss distance filter system for suppressing false resolution alerts, October 1996. U.S. Patent 5,566,074.

4. James Kuchar and Lee Yang. A review of conflict detection and resolution modeling methods. *IEEE Transactions on Intelligent Transportation Systems*, 1(4):179–189, December 2000.

5. César Muñoz, Anthony Narkawicz, and James Chamberlain. A TCAS-II resolution advisory detection algorithm. In *Proceedings of the AIAA Guidance Navigation, and Control Conference and Exhibit 2013, AIAA-2013-4622*, Boston, Massachusetts, 2013.

6. Anthony J. Narkawicz, César A. Muñoz, Jason M. Upchurch, James P. Chamberlain, and María C. Consiglio. A well-clear volume based on time to entry point. Technical Memorandum NASA/TM-2014-218155, NASA, Langley Research Center, Hampton VA 23681-2199, USA, January 2014.

7. S. Owre, J. Rushby, and N. Shankar. PVS: A prototype verification system. In Deepak Kapur, editor, *Proc. 11th Int. Conf. on Automated Deduction*, volume 607 of *Lecture Notes in Artificial Intelligence*, pages 748–752. Springer-Verlag, June 1992.

8. RTCA SC-147. RTCA-DO-185B, Minimum operational performance standards for traffic alert and collision avoidance system II (TCAS II), July 2009.

9. J. Tadema, E. Theunissen, and K.M. Kirk. Self separation support for UAS. In *AIAA Infotech@Aerospace 2010*, number AIAA-2010-3460, Atlanta, GA, USA, April 2010.

10. U.S. Department of Transportation Federal Aviation Adminstration. *Introduction to TCAS II Version 7.1*, February 2011.

11. Unmanned Vehicle Systems International (UVSI). *RPAS: Remoted Piloted Aircraft Systems - The Global Perspective*. Blyenburgh & Co., Paris, France, 10th edition, June 2012. uvs-info.com.

1. REPORT DATE *(DD-MM-YYYY)*	2. REPORT TYPE	3. DATES COVERED *(From - To)*
01-06-2014	Technical Memorandum	

4. TITLE AND SUBTITLE	5a. CONTRACT NUMBER
Analysis of Well-Clear Boundary Models for the Integration of UAS in the NAS	
	5b. GRANT NUMBER
	5c. PROGRAM ELEMENT NUMBER

6. AUTHOR(S)	5d. PROJECT NUMBER
Upchurch, Jason M.; Munoz, Cesar A.; Narkawicz, Anthony J.; Chamberlain, James P.; Consiglio, Maria C.	
	5e. TASK NUMBER
	5f. WORK UNIT NUMBER
	425425.04.01.07.02

7. PERFORMING ORGANIZATION NAME(S) AND ADDRESS(ES)	8. PERFORMING ORGANIZATION REPORT NUMBER
NASA Langley Research Center Hampton, VA 23681-2199	L-20407

9. SPONSORING/MONITORING AGENCY NAME(S) AND ADDRESS(ES)	10. SPONSOR/MONITOR'S ACRONYM(S)
National Aeronautics and Space Administration Washington, DC 20546-0001	NASA
	11. SPONSOR/MONITOR'S REPORT NUMBER(S)
	NASA/TM-2014-218280

12. DISTRIBUTION/AVAILABILITY STATEMENT
Unclassified - Unlimited
Subject Category 03
Availability: NASA CASI (443) 757-5802

13. SUPPLEMENTARY NOTES

14. ABSTRACT

The FAA-sponsored Sense and Avoid Workshop for Unmanned Aircraft Systems (UAS) defines the concept of sense and avoid for remote pilots as "the capability of a UAS to remain well clear from and avoid collisions with other airborne traffic." Hence, a rigorous definition of well clear is fundamental to any separation assurance concept for the integration of UAS into civil airspace. This paper presents a family of well-clear boundary models based on the TCAS II Resolution Advisory logic. Analytical techniques are used to study the properties and relationships satisfied by the models. Some of these properties are numerically quantified using statistical methods.

15. SUBJECT TERMS

National airspace; Safety; Separation assurance; Unmanned aircraft systems; Well-Clear boundary; Well-Clear violation

16. SECURITY CLASSIFICATION OF:			17. LIMITATION OF ABSTRACT	18. NUMBER OF PAGES	19a. NAME OF RESPONSIBLE PERSON
a. REPORT	b. ABSTRACT	c. THIS PAGE			STI Help Desk (email: help@sti.nasa.gov)
U	U	U	UU	27	19b. TELEPHONE NUMBER *(Include area code)* (443) 757-5802